First Generation Interferometers

Barry C. Barish

California Institute of Technology
Pasadena, CA 91125

Abstract. The status and plans for the first generation long baseline suspended mass interferometers TAMA, GEO, LIGO and Virgo are presented, as well as the expected performances.

INTRODUCTION

The effect of the propagating gravitational wave is to deform space in a quadrupolar form. The characteristics of the deformation are indicated in Fig. 1.

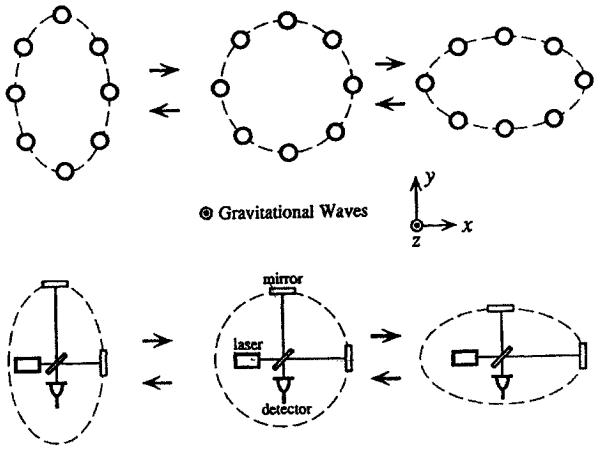

FIGURE 1. The effect of gravitational waves for one polarization is shown at the top on a ring of free particles. The circle alternately elongates vertically while squashing horizontally and vice versa with the frequency of the gravitational wave. The detection technique of interferometry being employed in the new generation of detectors is indicated in the lower figure. The interferometer measures the difference in distance in two perpendicular directions, which if sensitive enough could detect the passage of a gravitational wave

For an astrophysical source, one can estimate the frequency of the emitted gravitational wave. An upper limit on the gravitational wave source frequency can be estimated from the Schwarzshild radius $2GM/c^2$ of the radiated object. We do not

CP575, *Astrophysical Sources for Ground-Based Gravitational Wave Detectors,* edited by J. M. Centrella

expect strong emission for periods shorter than the light travel time $4\pi GM/c^3$ around its circumference. From this we can estimate the maximum frequency as about 10^4 *Hz* for a solar mass object. Of course, the frequency can be much lower as illustrated by the 8 hour period of PSR1916+13, which is emitting gravitational radiation. Frequencies in the higher frequency range $1Hz < f < 10^4$ *Hz* are potentially reachable using detectors on the earth's surface, while the lower frequencies require putting an instrument into space. The physics goals of the terrestrial detectors and the LISA space mission are complementary, much like different frequency bands are used in observational astronomy for electromagnetic radiation

The strength of a gravitational wave signal depends crucially on the quadrupole moment of the source. We can roughly estimate how large the effect could be from astrophysical sources. If we denote the quadrupole moment of the mass distribution of a source by Q, a dimensional argument, along with the assumption that gravitational radiation couples to the quadrupole moment yields:

$$h \sim \frac{G\ddot{Q}}{c^4 r} \sim \frac{G(E_{kin}^{non-symm.}/c^2)}{c^2 r} \tag{1}$$

where G is the gravitational constant and $E_{kin}^{non-symm.}$ is the non-symmetrical part of the kinetic energy.

For the purpose of estimation, let us consider the case where one solar mass is in the form of non-symmetric kinetic energy. Then, at a distance of the Virgo cluster we estimate a strain of $h \sim 10^{-21}$. This is a good guide to the largest signals that might be observed. At larger distances or for sources with a smaller quadrupole component the signal will be weaker

LONG BASELINE INTERFEROMETRY

A Michelson interferometer operating between *freely suspended* masses is ideally suited to detect the antisymmetric (compression along one dimension and expansion along an orthogonal one) distortions of space induced by the gravitational waves as was illustrated in figure 1. Other optical configurations or interferometer schemes, like a Sagnac, might also be used and could have advantages, but the present generation of interferometers discussed here are of the Michelson type.

The simplest configuration, a white light (equal arm) Michelson interferometer is instructive in visualizing many of the concepts. In such a system the two interferometer arms are identical in length and in the light storage time. Light brought to the beam splitter is divided evenly between the two arms of the interferometer. The light is transmitted through the splitter to reach one arm and reflected by the splitter to reach the other arm. The light traverses the arms and is returned to the splitter by the distant arm mirrors. The roles of reflection and transmission are interchanged on this return and, furthermore, due to the Fresnel laws of E & M the return reflection is accompanied by a sign reversal of the optical electric field. When the optical electric fields that have come from the two arms are recombined at the beam splitter, the beams that were treated to a reflection (transmission) followed by a transmission

(reflection) emerge at the antisymmetric port of the beam splitter while those that have been treated to successive reflections (transmissions) will emerge at the symmetric port.

In a simple Michelson configuration the detector is placed at the antisymmetric port and the light source at the symmetric port. If the beam geometry is such as to have a single phase over the propagating wavefront (an idealized uniphase plane wave has this property as does the Gaussian wavefront in the lowest order spatial mode of a laser), then, providing the arms are equal in length (or their difference in length is a multiple of 1/2 the light wavelength), the entire field at the antisymmetric port will be dark. The destructive interference over the entire beam wavefront is complete and all the light will constructively recombine at the symmetric port. The interferometer acts like a light valve sending light to the antisymmetric or symmetric port depending on the path length difference in the arms.

If the system is balanced so that no light appears at the antisymmetric port, the gravitational wave passing though the interferometer will disturb the balance and cause light to fall on the photodetector at the dark port. This is the basis of the detection of gravitational waves in a suspended mass interferometer. In order to obtain the required sensitivity, the arms of the interferometer must be long.

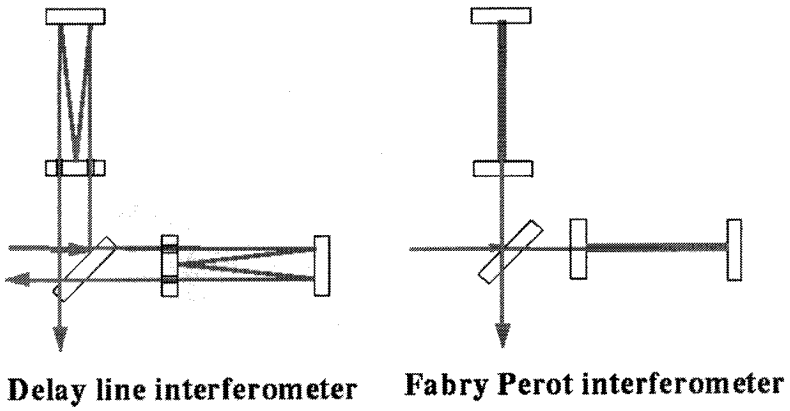

FIGURE 2. Folded optical configurations for interferometer. The arrangement on the left is called a delay line interferometer and the one on the right using a resonant cavity is a Fabry Perot interferometer. The GEO600 interferometer is a delay line interferometer, while the all the other long baseline interferometers use Fabry Perot resonant cavities.

The amount of motion of the arms to produce an intensity change at the photodetector depends on the optical length of the arm; the longer the arm the greater is the change in length up to a length that is equal to 1/2 the gravitational wave wavelength. Equivalently the longer the interaction of the light with the gravitational wave, up to 1/2 the period of the gravitational wave, the larger is the optical phase shift due to the gravitational wave and thereby the larger is the intensity change at the photodetector. The initial long baseline interferometers, besides having long arms also

will fold the optical beams in the arms in optical cavities or delay lines to gain further increase in the path length or equivalently in the interaction time of the light with the gravitational wave (Fig. 2). The initial LIGO interferometers will store the light about 50 times longer than the beam transit time in an arm. (A light storage time of about 1 millisecond.)

Another feature employed in these interferometers is to increase the change in intensity due to a phase change at the antisymmetric port by making the entire interferometer into a resonant optical storage cavity. The fact that the interferometer is operated with no light emerging at the antisymmetric port and all the light that is not lost in the mirrors or scattered out of the beam returns toward the light source via the symmetric port, makes it possible to gain a significant factor by placing another mirror between the laser and the symmetric port and 'reuse the light'. This technique is general referred to as power recycling. By choosing this mirror's position properly and by making the transmission of this mirror equal to the optical losses inside the interferometer, one can "match" the losses in the interferometer to the laser so that no light is reflected back to the laser. As a consequence, the light circulating in the interferometer is increased by the reciprocal of the losses in the interferometer. This is equivalent to increasing the laser power and does not affect the frequency response of the interferometer to a gravitational wave. The power gain achieved by this scheme can be a factor of 10 or even 100.

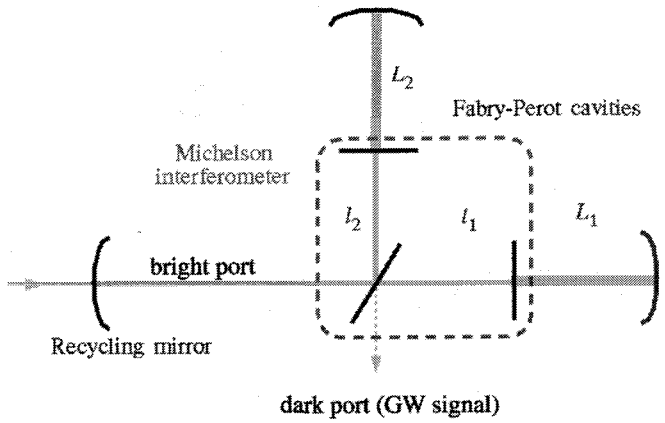

FIGURE 3. The optical configuration of a Michelson interferometer with Fabry-Perot arms is shown. A relative change in length of the two arms causes a phase shift destroying the destructive interference and the dark port detects a signal

The system just described is called a power recycled Fabry-Perot Michelson interferometer and it is this type of configuration that will be used in the initial interferometers (Fig. 3). There are many other possible types of interferometer configurations, such as narrow band interferometers with the advantage of increased sensitivity in a narrow frequency range. This can be accomplished by adding yet

another mirror in the output port and is generally called signal recycling. Such interferometers are planned for future versions of the various interferometers facilities and the GEO600 interferometer has already incorporated this capability.

The interferometer parameters of the new set of detectors just being brought online have been chosen such that the initial sensitivity will be consistent both with the dimensional arguments given above and with estimates needed for possible detection of known sources. Although the rate for these sources are very uncertain, large increases in sensitivity are anticipated as the detectors are improved. This is because the planned incremental improvements in sensitivity correspond to the cube of that improvement in the event rate, which scales as the volume searched.

THE INTERFEROMETER NOISE FLOOR

The success of the detector ultimately will depend on how well we one can to control the noise in the measurement of these small strains. Noise is broadly but also usefully categorized in terms of those phenomena which limit the ability to sense and register the small motions (sensing noise limits) and those that perturb the masses by causing small motions (random force noise). Eventually one reaches the ultimate limiting noise, the quantum limit, which combines the sensing noise with a random force limit. This orderly and intellectually satisfying categorization presumes that one is careful enough as experimenters in the execution of the experiment that one has not produced less fundamental, albeit, real noise sources that are caused by faulty design or poor implementation. These might be referred to as technical noise sources and in real life these have often been the impediments to progress and mask the limiting noise sources of the interferometer. The primary noise sources for the initial detectors are illustrated in Fig. 4, where the estimated levels of the various noise sources are shown for LIGO. The other interferometers have similar curves with some difference in detail due to the different trade-offs that have been made.

In order to control the technical noise sources, extensive use is made of two concepts. The first is the technique of modulating the signal to be detected at frequencies far above the 1/f noise due to the drift and gain instabilities experienced in all instruments. For example, the optical phase measurement to determine the motion of the fringe is carried out at radio frequency rather than near DC. Thereby, the low frequency amplitude noise in the laser light will not directly perturb the measurement of the fringe position. (The low frequency noise still will cause radiation pressure fluctuations on the mirrors through the asymmetries in the interferometer arms.) A second concept is to apply feedback to physical variables in the experiment to control the large excursions at low frequencies and to provide damping. The variable is measured through the control signal required to hold it stationary. Here a good example is the position of the interferometer mirrors at low frequency. The interferometer fringe is maintained at a fixed phase by holding the mirrors at fixed positions at low frequencies. Feedback forces to the mirrors effectively hold the mirrors "rigidly". In the initial LIGO interferometers the forces are provided by permanent magnet/coil combinations. The mirror motion that would have occurred is then read in the control signal required to hold the mirror.

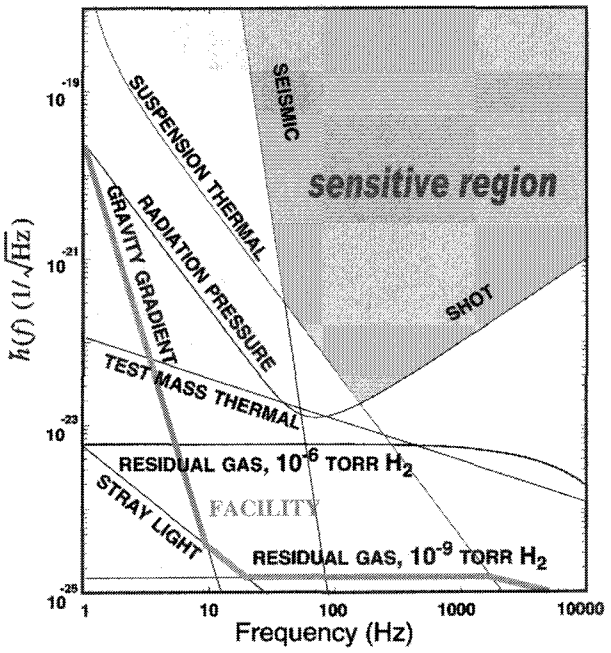

Figure 4. Limiting noise sources for the initial LIGO detectors. Note that the interferometer is limited by different sources at low frequency (e.g. seismic), middle frequencies by suspension thermal noise, and at high frequencies by shot noise (or photo statistics). Lurking below are many other potential noise sources

Great care must be taken to control the technical noise sources. In order to test and understand the sensitivity and limiting noise, extensive tests have been performed with a 40 meter LIGO prototype interferometer on the Caltech campus. This interferometer essentially has all the pieces and the optical configuration used in LIGO, so represents a good place to understand noise and performance before the full-scale LIGO interferometers are in operation. The 40 m prototype device has achieved a displacement sensitivity of $h \sim 10^{-19}\ m/Hz^{1/2}$, which is close to the displacement sensitivity that is required in the 4 km LIGO interferometers. Fig. 5 shows the measured noise curve in this prototype instrument. The modeled noise sources are shown and for the most part are a good representation of the observed performance, including the most of the line structures that are due to wire resonances and other such sources. The same model has been used to determine the expected sensitivity curve for LIGO.

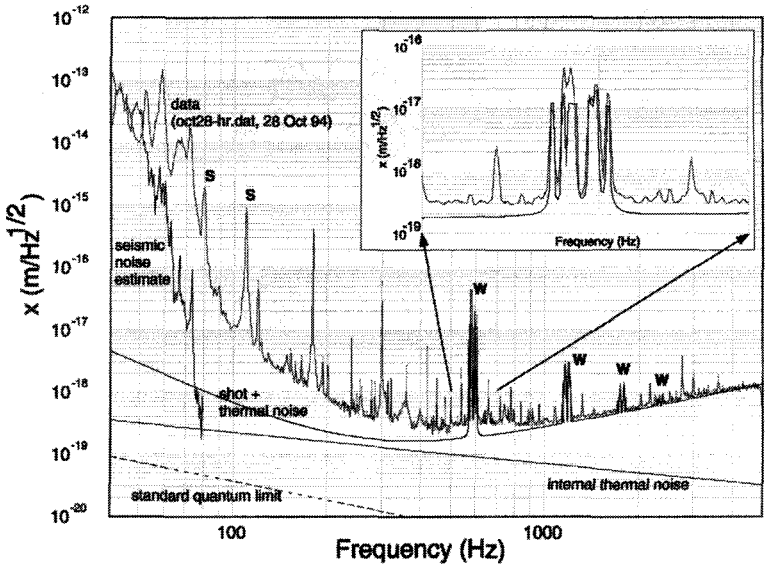

Figure 5. The displacement noise measured in the 40m suspended mass interferometer LIGO prototype on the Caltech campus. The general shape and level are well simulated by our understanding of the limiting noise sources - seismic noise at the lowest frequencies, suspension thermal noise at the intermediate frequencies, and shot noise at the highest frequencies. Also, the primary line features are understood as various resonances in the suspension system.

STATUS OF THE INTERFEROMETER PROJECTS

TAMA300

The first of the new generation of interferometers (TAMA300) has begun initial operation over the past year. TAMA300 is a Fabry-Perot Michelson interferometer with arm lengths of 300m. The site is at the National Astronomical Observatory of Japan (Tokyo, Mitaka). The interferometer uses a 10W injection-locked LD-pumped Nd:YAG laser and employs a 10m-length ring-type cavity mode cleaner to condition the input beam. The interferometer is designed for power recycling with gain of x10, which has not yet been employed. The design sensitivity is $h_{RMS} = 3 \times 10^{-21}$. The best sensitivity achieved to date is a displacement noise of about $4\ 10^{-18}$ m/Hz$^{1/2}$, corresponding to a strain sensitivity of approximately $h \sim 1\ 10^{-20}$/Hz$^{1/2}$.

The improvement of the noise curve as the interferometer has been commissioned over the past year is shown in Fig. 6. The figure shows the improvements in the noise curve during the first eight months of operation, and Fig. 7 shows a break down of the main contributors to the curve from various noise sources.

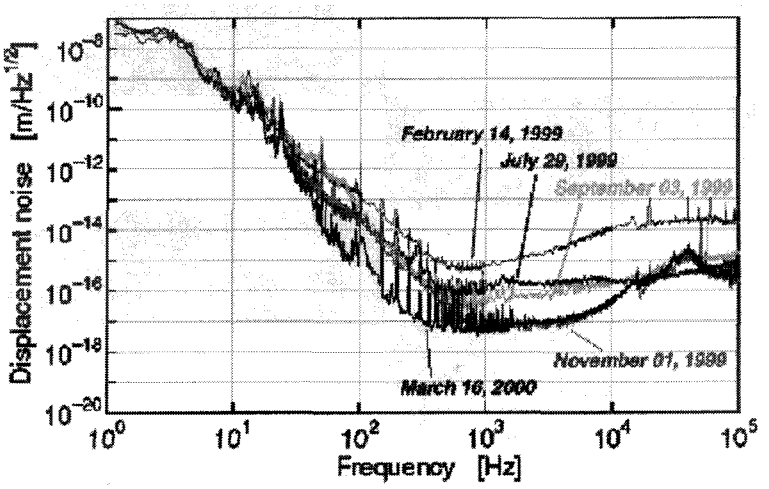

FIGURE 6. The performance of the TAMA300 interferometer, the first of the new generation of interferometers to begin operation is shown. The top curve shows the dramatic improvement from Sept 1999 when the interferometer established its first noise curves until March 16, 2000 when the noise curve had been improved by about 4 orders of magnitude.

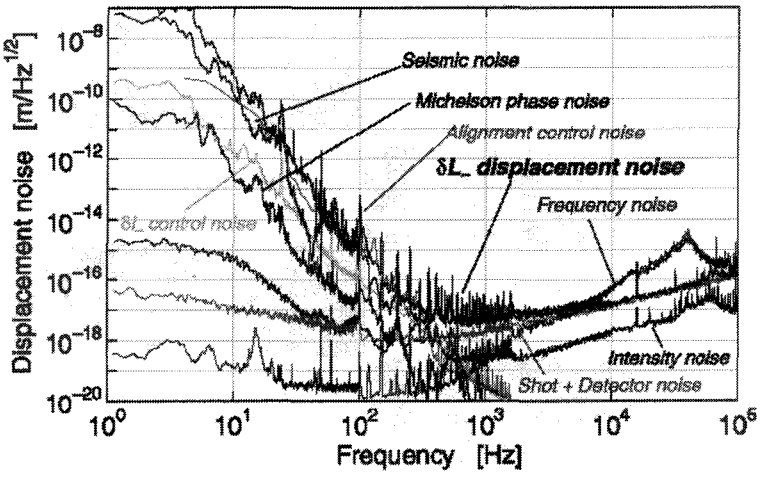

Figure 7. For the March run the noise in TAMA has been broken up into its various components. Improvements are planned in the near future to improve the seismic and other dominant noise sources

GEO600

The GEO600 interferometer facility, a U.K.- German collaboration is located in Hanover, Germany. It has 600m long arms and incorporates signal recycling and an advanced suspension system. The triple suspension system (fig 8) consists of an upper

mass/cantilever spring and intermediate mass and a test mass / reaction mass combination. The controls are applied to the upper masses to reduce noise. 4 x 180mm silica wires are welded to the silica test mass. GEO construction is complete and commissioning is underway. The vacuum system is operational, central optics are installed and a long arm test of the interferometer is in progress.

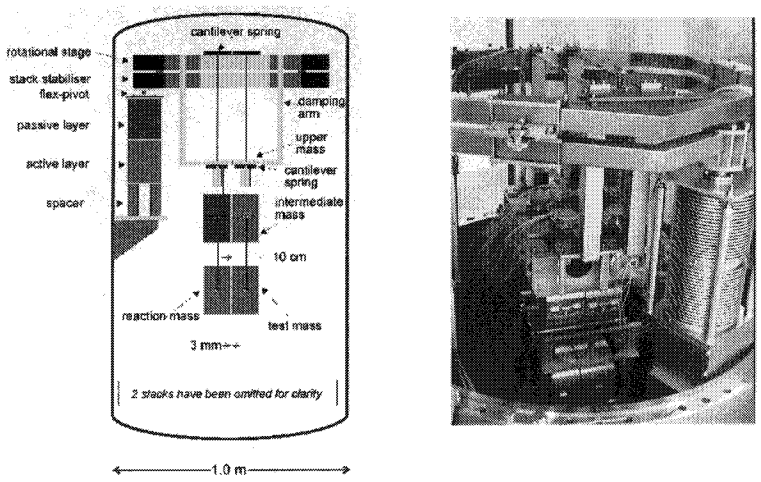

Figure 8. On the left is a schematic of the GEO600 triple suspension system, which employs drawn silica wires bonded to the test masses. The controls are applied only to the upper masses to reduce noise.

LIGO

LIGO at Hanford has both a half-length (2km) and a full-length (4km) interferometer installed in the same vacuum chamber. The extra constraint of requiring a half-size signal in the shorter interferometer will be used to eliminate common noise and lower the singles rate in the coincidence between the sites. Over the past year, the long 2 km arm cavities were locked one at a time for typical few hour times, at which point lock was lost due to tidal effects. The electronics to compensate for tidal effects had not yet been installed

Following the locking of the long arms early in 2000, attention was shifted to the power-recycled Michelson part of the interferometer, formed by the input mirrors, as well as the beam splitter and the recycling mirror. To make LIGO as sensitive as possible, one wants as much light as possible returning to the beam splitter. This occurs when the recycling mirror is placed at the correct distance from the beam splitter, 'trapping' the reflected light in the Michelson interferometer. This causes the laser light in the interferometer to build up to a high level. For the full system, recycling will cause the light to build up by about a factor of thirty. When this build

up occurs, the power-recycled Michelson interferometer is resonating. Such a resonant state was achieved with the short arm system during the summer.

The final step was to lock the full interferometer, achieving 'first lock' in the LIGO interferometers. This was achieved this fall for short lock periods as shown in Fig. 9. Robust locking is now achieved in the recombined configuration and a very successful one-week engineering test run in his configuration was carried out this month. A variety of electronic dynamic range and gain issues are presently limiting the stability of the lock for the power recycled configuration, which will be the focus of the activities in the coming months, as well as the commissioning of the interferometer at Livingston. The first coincidence test running between the two sites is planned for summer 2001.

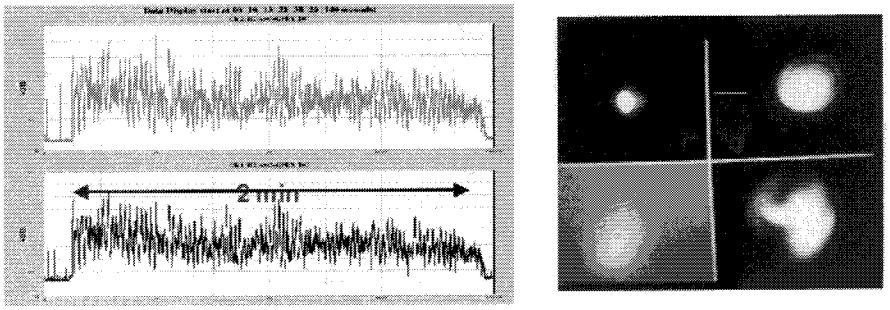

FIGURE 9. Data recording the first lock in LIGO of the full power recycled Michelson Fabry-Perot interferometer. The traces on the left show a 2 minute stretch where lock was held stable, while the figure on the right shows images of the locked beam at the recycling mirror (bottom left), beam splitter (bottom right); and at the end test masses of each 2km arm (top images). The large contrast in the top photos is an indication of the intensity of the resonating beam in the arms. The difference in sizes of the images in the two arms is an artifact of the magnification of the cameras.

Virgo

The Virgo Experiment is a French-Italian collaboration and is located at Cascina, Italy not far from Pisa. The infrastructure housing the central interferometer is complete and the sophisticated seismic-suspension system is being implemented. This Virgo seismic-suspension system, which is designed to give the best sensitivity of the new generation of detectors at low frequencies, is illustrated in Fig. 10, as well as the performance from a full-scale prototype. All four long suspensions for the entire central interferometer are scheduled for completion by the end of 2000.

The laser, input optics and mode cleaner have been installed and testing of this system, which will lead to a commissioned short arm version of Virgo are planned while the long arms are under construction. The first long arm is scheduled to be completed by 2002, as well as the large optics. The full long baseline interferometer is scheduled to begin operations by the end of 2002.

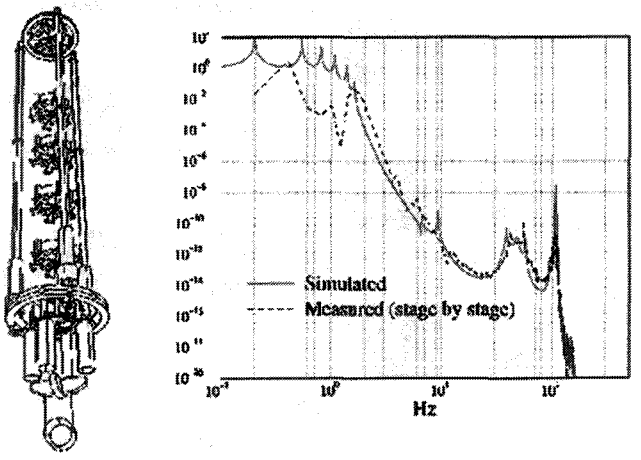

Figure 10. The Virgo long suspension with five intermediate stages is shown on the left. The figure on the right shows the suspension vertical transfer function measured and simulated (prototype).

AIGO

Initial steps toward a long baseline interferometer facility have been initiated near Perth, Australia. A collaboration of Australian Universities (ACIGA) is developing the facility, as well as actively collaborating with the other interferometer groups. The consortium is doing research on high power lasers, new optical configurations, suspensions, test masses, etc. The central facility for AIGO has been constructed and work is underway to build the central optics and a short arm interferometer as the first step toward the hope of eventually extending the arms to a long baseline interferometer to be used in conjunction with those being developed in the northern hemisphere. In addition, an R & D program to test optics at the high powers envisioned for second-generation interferometers is being planned.

CONCLUSIONS

The first generation interferometers having sensitivities that should allow searches with $h \sim 10^{-21}$ are becoming operational. These will be the first experimental searches that approach the sensitivity where detection of gravitational waves is plausible. The design sensitivities of the major interferometer projects are shown in Fig. 11. In addition to the anticipated 'stand-alone' searches using each of these detectors, discussions and preparations are underway to bring the data together from the different detectors to do coincidence work to both improve overall sensitivity and confidence in detection. Significant improvements to these detectors are anticipated to be initiated in about 5 years that should improve the sensitivity to $h \sim 10^{-22}$.

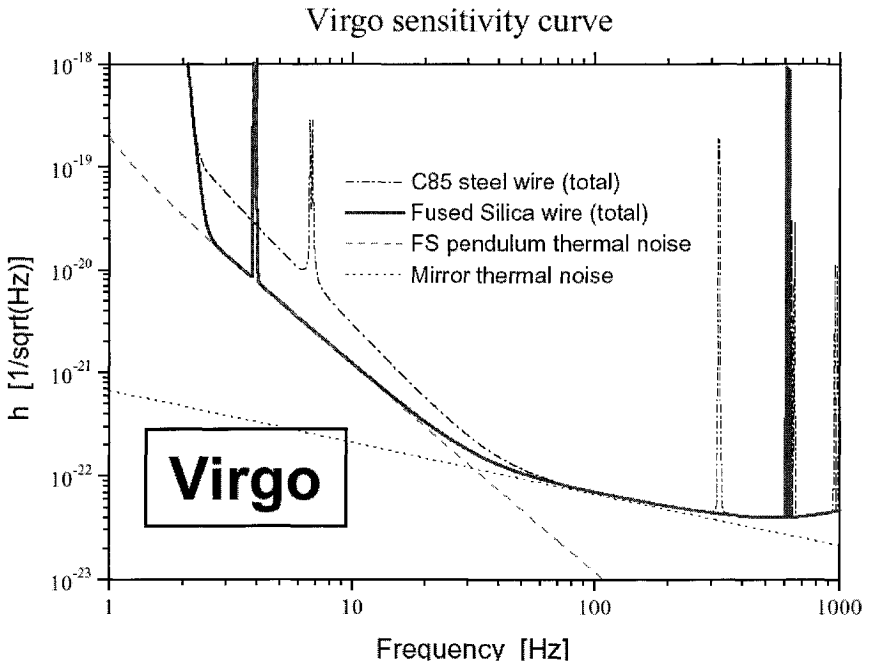

FIGURE 11. The design sensitivities of the Virgo interferometer is shown. This is illustrative of what will be obtained in the next few year from the new generation of detectors.

REFERENCES

1. LIGO http://www.ligo.caltech.edu/
2. Virgo: http://www.virgo.infn.it/
3. GEO600 http://www.geo600.uni-hannover.de/
4. TAMA http://tamago.mtk.nao.ac.jp/
5. AIGO http://www.gravity.uwa.edu.au/AIGO/AIGO.html